POLYPUBLIE
Polytechnique Montréal

POLYTECHNIQUE MONTRÉAL
UNIVERSITÉ D'INGÉNIERIE

Titre: Title: Carboplatin sensitivity in epithelial ovarian cancer cell lines: The impact of model systems

Auteurs: Authors: Shannon M. Hawkins, Bishnubrata Patra, Muhammad Abdul Lateef, Melica Nourmoussavi Brodeur, Hubert Fleury, Euridice Carmona, Benjamin Péant, Diane Provencher, Anne-Marie Mes-Masson, & Thomas Gervais

Date: 2020

Type: Article de revue / Article

Référence: Citation: Hawkins, S. M., Patra, B., Lateef, M. A., Brodeur, M. N., Fleury, H., Carmona, E., Péant, B., Provencher, D., Mes-Masson, A.-M., & Gervais, T. (2020). Carboplatin sensitivity in epithelial ovarian cancer cell lines: The impact of model systems. PLOS One, 15(12), 17 pages. https://doi.org/10.1371/journal.pone.0244549

Document en libre accès dans PolyPublie
Open Access document in PolyPublie

URL de PolyPublie: PolyPublie URL: https://publications.polymtl.ca/9359/

Version: Version officielle de l'éditeur / Published version
Révisé par les pairs / Refereed

Conditions d'utilisation: Terms of Use: Creative Commons Attribution 4.0 International (CC BY)

Document publié chez l'éditeur officiel
Document issued by the official publisher

Titre de la revue: Journal Title: PLOS One (vol. 15, no. 12)

Maison d'édition: Publisher: PLOS

URL officiel: Official URL: https://doi.org/10.1371/journal.pone.0244549

Mention légale: Legal notice: © 2020 Patra et al. This is an open access article distributed under the terms of the Creative Commons Attribution License, which permits unrestricted use, distribution, and reproduction in any medium, provided the original author and source are credited.

Ce fichier a été téléchargé à partir de PolyPublie, le dépôt institutionnel de Polytechnique Montréal
This file has been downloaded from PolyPublie, the institutional repository of Polytechnique Montréal

https://publications.polymtl.ca

PLOS ONE

RESEARCH ARTICLE

Carboplatin sensitivity in epithelial ovarian cancer cell lines: The impact of model systems

Bishnubrata Patra[1,2☯], Muhammad Abdul Lateef[2☯], Melica Nourmoussavi Brodeur[2], Hubert Fleury[2], Euridice Carmona[2], Benjamin Péant[2], Diane Provencher[2,3], Anne-Marie Mes-Masson[2,4]*, Thomas Gervais[1,2]*

1 Department of Engineering Physics and Institute of Biomedical Engineering, École Polytechnique de Montréal, Montréal, QC, Canada, **2** Centre de Recherche du Centre Hospitalier de l'Université de Montréal (CRCHUM) and Institut du Cancer de Montréal, Montréal, QC, Canada, **3** Division of Gynecologic Oncology, Université de Montréal, Montréal, QC, Canada, **4** Department of Medicine, Université de Montréal, Montréal, QC, Canada

☯ These authors contributed equally to this work.
* thomas.gervais@polymtl.ca (TG); anne-marie.mes-masson@umontreal.ca (AMMM)

Check for updates

OPEN ACCESS

Citation: Patra B, Lateef MA, Brodeur MN, Fleury H, Carmona E, Péant B, et al. (2020) Carboplatin sensitivity in epithelial ovarian cancer cell lines: The impact of model systems. PLoS ONE 15(12): e0244549. https://doi.org/10.1371/journal.pone.0244549

Editor: Shannon M. Hawkins, Indiana University School of Medicine, UNITED STATES

Received: October 8, 2020

Accepted: December 13, 2020

Published: December 31, 2020

Copyright: © 2020 Patra et al. This is an open access article distributed under the terms of the Creative Commons Attribution License, which permits unrestricted use, distribution, and reproduction in any medium, provided the original author and source are credited.

Data Availability Statement: All relevant data are within the manuscript and its Supporting Information files.

Funding: This work was supported by grants from the Cancer Research Society partnered with Ovarian Cancer Canada (#20103 to AMMM, DP and TG), the Canadian Cancer Society Research Institute (#702952 to AMMM, DP and TG), the National Science and Engineering Research Council of Canada (#RGPIN-06409 to TG), and the ICM (Fonds Défi Spyder and Anne-Marie Chagnon to

Abstract

Epithelial ovarian cancer (EOC) is the most lethal gynecologic malignancy in North America, underscoring the need for the development of new therapeutic strategies for the management of this disease. Although many drugs are pre-clinically tested every year, only a few are selected to be evaluated in clinical trials, and only a small number of these are successfully incorporated into standard care. Inaccuracies with the initial *in vitro* drug testing may be responsible for some of these failures. Drug testing is often performed using 2D monolayer cultures or 3D spheroid models. Here, we investigate the impact that these different *in vitro* models have on the carboplatin response of four EOC cell lines, and in particular how different 3D models (polydimethylsiloxane-based microfluidic chips and ultra low attachment plates) influence drug sensitivity within the same cell line. Our results show that carboplatin responses were observed in both the 3D spheroid models tested using apoptosis/cell death markers by flow cytometry. Contrary to previously reported observations, these were not associated with a significant decrease in spheroid size. For the majority of the EOC cell lines (3 out of 4) a similar carboplatin response was observed when comparing both spheroid methods. Interestingly, two cell lines classified as resistant to carboplatin in 2D cultures became sensitive in the 3D models, and one sensitive cell line in 2D culture showed resistance in 3D spheroids. Our results highlight the challenges of choosing the appropriate preclinical models for drug testing.

Introduction

Epithelial ovarian cancer (EOC) is the 5th cause of cancer-related deaths in North American women with a 5-year survival of 45% [1]. The standard front-line treatment for EOC includes cytoreductive surgery and treatment with platinum DNA alkylating agents such as carboplatin or cisplatin combined with the anti-microtubule drug paclitaxel [2]. Although initial response

DP). This research was conducted as part of the TransMedTech Institute's activities and thanks, in part, to funding from the Canada First Research Excellence Fund. Ovarian tumor banking was supported by Ovarian Cancer Canada (OCC) and by the Banque de tissus et de données of the Réseau de recherche sur le cancer of the Fonds de recherche du Québec - Santé (FRQS) affiliated with the Canadian Tumor Repository Network (CTRNet). AMMM and DP are researchers of the CRCHUM/ICM, which receive support from the FRQS. MAL was supported by a MITACS fellowship. HF received the ICM Michèle St-Pierre Bursary and the ICM Canderel fellowship. The funders had no role in study design, data collection and analysis, decision to publish, or preparation of the manuscript. There was no additional external funding received for this study.

Competing interests: The authors have declared that no competing interests exist.

rates are high (>70%), the disease eventually recurs in most patients, who will then develop chemoresistance [2–4]. To improve EOC survival, new therapies and their combinations are under investigation, and preclinical models are used to test their efficacy prior to eventual human trials. Because of time and cost efficiency, these models are often in the form of 2D or 3D *in vitro* assays. However, optimizing and translating the results seen in 2D *in vitro* models to an *in vivo* response is challenging, as these models do not take into account important tumor characteristics such as hypoxia, drug transport restriction, extra cellular matrix (ECM), anchorage-independent growth as well as interactions with other cell types in the tumor, including stroma/fibroblast and immune cells [5–8]. Alternatively, 3D spheroid models have been proposed as an attractive alternative as they are thought to more closely resemble the tumor tissue architecture [9–11].

There are several methods to prepare 3D spheroids from cell lines (reviewed elsewhere [11, 12]) including hanging-droplets [13–16], rotating wall vessel cultures [14, 17], and ultra-low attachment (ULA) 96-well round-bottom plates [11, 18, 19]. In ovarian cancer, several groups have described the capacity of EOC cell lines to form spheroids by different methodologies [20–26], including our work using hanging droplets [16, 27–29]. These different techniques each have their own challenges. On one hand, hanging-droplet spheroids take longer to form, are difficult to manipulate for spheroid transfer steps, and they present a challenge for experiments requiring medium changes [30, 31] or treatments. On the other hand, spheroids formed in ULA plates can be readily used in high-throughput assays [18, 19] but many cell lines do not form spheroids under these conditions. Considering the importance of the tissue microenvironment in the establishment of 3D models, components of the ECM have been used to assist spheroid formations [11]. Matrigel, consisting of collagen type IV, perlecan/heparin sulfate proteoglycan 2 and laminin, is one of the most commonly used ECM mimics [11, 32] and has been shown to improve spheroid formation in ULA plates for cell lines that otherwise would not have the capacity to aggregate [18, 19]. More recently, many bioengineered microfluidic devices have been developed and shown to be effective in forming spheroids [33–39]. In addition, the use of these microfluidic devices has gained popularity as a 3D model system for drug screening [12, 33–44]. In ovarian cancer, our group has been a pioneer in the application of this technology to evaluate drug response in EOC cell lines [37, 38, 41].

Although several studies have compared the chemosensitivity of ovarian cancer cell lines grown as monolayers with 3D-spheroid cultures [18, 41, 45, 46], little is known about the impact that different 3D spheroid model systems have on their sensitivity. In the present study, we investigated the ability of four different EOC cell lines to form 3D spheroids following different methodologies (hanging-droplets, ULA plates and microfluidic chips), and their carboplatin sensitivity in monolayer culture versus spheroids formed within microfluidic devices or round-bottom ULA plates (the latter using Matrigel as an ECM) (Fig 1). Response was measured by flow cytometry for apoptosis/cell death and spheroid size measurement. Our results show that spheroid formation of EOC cell lines is significantly faster and more uniform in polydimethylsiloxane (PDMS) microfluidic devices and Matrigel-assisted ULA plates than in hanging-droplets or ULA plates without Matrigel. Carboplatin responses were observed in both 3D spheroid models using flow cytometric analysis, but no significant decrease in spheroid size was detected. For the majority of the EOC cell lines (3 out of 4) a similar response to carboplatin treatment was observed by both spheroid methods. Interestingly, two cell lines classified as resistant to carboplatin in 2D cultures responded as sensitive in 3D models, and one sensitive cell line in 2D culture showed resistance in the 3D spheroids. Our results highlight the challenges in choosing appropriate pre-clinical models for empirical drug testing.

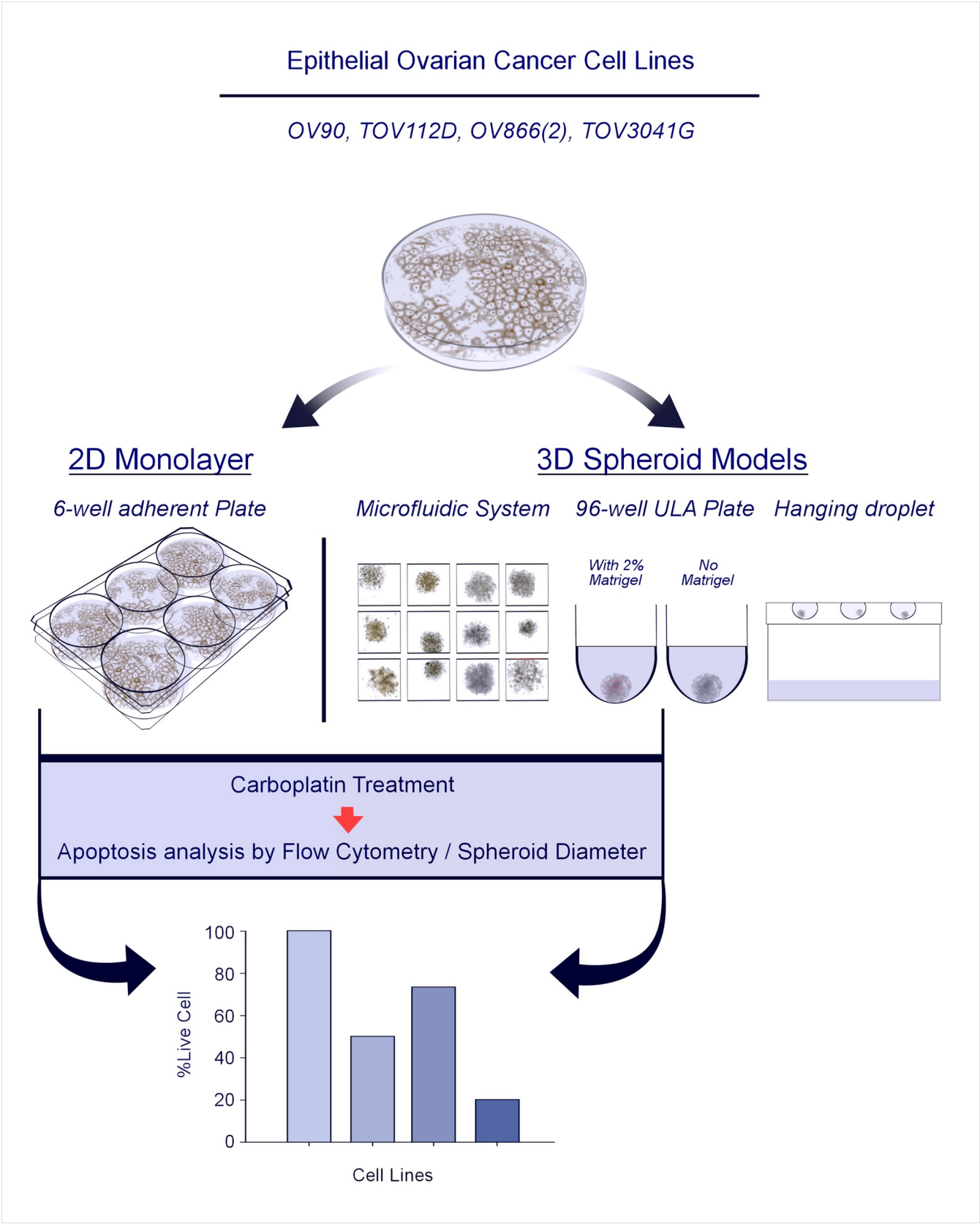
Epithelial Ovarian Cancer Cell Lines
OV90, TOV112D, OV866(2), TOV3041G
2D Monolayer
3D Spheroid Models
6-well adherent Plate
Microfluidic System
96-well ULA Plate
Hanging droplet
With 2% Matrigel
No Matrigel
Carboplatin Treatment
Apoptosis analysis by Flow Cytometry / Spheroid Diameter
%Live Cell
100
80
60
40
20
0
Cell Lines

Fig 1. Schematic illustration of the study strategy. For each cell line used, 3D spheroid formation was evaluated by four different methods, i.e., PDMS-based microfluidic systems, ultra-low attachment (ULA) plates in the presence or not of 2% Matrigel, and hanging droplets. The two most effective 3D spheroid methods (microfluidic chips and Matrigel-assisted ULA plates) were used to define carboplatin sensitivity of each cell line that was then compared to responses in the 2D monolayer assay.

https://doi.org/10.1371/journal.pone.0244549.g001

Materials and methods

Cell lines

Four different human EOC cell lines were used in this study, TOV3041G, TOV112D, OV90 and OV866(2) (all BRCA1/2 wild-type). Three cell lines [TOV112D, OV90, OV866(2)] are classified as resistant to carboplatin therapy in 2D culture as measured by clonogenic assay, and one (TOV3041G) is classified as sensitive (Table 1). These cell lines were derived in our laboratory from patient tumor (TOV) or ascites (OV) [27, 47] samples. All cell lines were authenticated at the beginning of this study using STR profiling by the McGill University Genome Center (Montreal, Canada). Cells were cultured in complete OSE medium (Wisent, QC, Canada) supplemented with 10% fetal bovine serum (Wisent), 2.5 μg/mL of amphotericin B (Wisent) and 50 μg/mL of gentamicin (Wisent). Cells were maintained in 100 mm petri dishes with 5% CO_2 at 37˚C.

Clonogenic survival assays

The IC_{50}'s for carboplatin, as determined by clonogenic survival assay, have previously been reported for TOV3041G, TOV112D, and OV866(2) [27, 28]. Carboplatin sensitivity for the OV90 cell line was determined in this study using the same clonogenic assay [27]. Briefly, cells were seeded in a 6-well plate at a density of 750 cells/well that allowed the formation of individual colonies. After seeding, cells were allowed to adhere for 16 hours in a 37˚C, 5% CO_2 incubator after which the medium was removed and replaced with OSE complete medium containing carboplatin (0–100μM) (Hospira Healthcare Corporation, Saint-Laurent, QC). Cells were incubated with the drug for 24 hours. The drug was then removed and OSE complete medium was added to each well. When colonies became visible at a 2X magnification plates were fixed with cold methanol and stained with a solution of 0.5% blue methylene (Sigma–Aldrich Inc., St. Louis, MO) in 50% methanol. Colonies were counted under a stereomicroscope and reported as percent of control. IC_{50} values were determined using Graph Pad Prism 5 software (GraphPad Software Inc., San Diego, CA). Each individual experiment was performed in triplicate and repeated three times.

Spheroid formation

Spheroids were formed using three different methods: hanging-droplet, PDMS-based microfluidic chips and ULA 96-well plates (with and without Matrigel). Hanging-droplet spheroids were generated as previously described [16]. Briefly, 16 μL droplets containing 4000 cells each were placed on the inside of the lid of a 150 mm cell culture plate. The lid was then gently

Table 1. Carboplatin sensitivity (IC_{50} by clonogenic assay) of the EOC cell lines used in this study.

	Carboplatin IC_{50} (μM)	Reference
TOV3041G	5.2 ± 1.1	Fleury et al. 2015
TOV112D	13.4	Letourneau et al. 2012
OV90	31.8 ± 5.4	This study
OV866(2)	32.1 ± 7.1	Fleury et al. 2015

https://doi.org/10.1371/journal.pone.0244549.t001

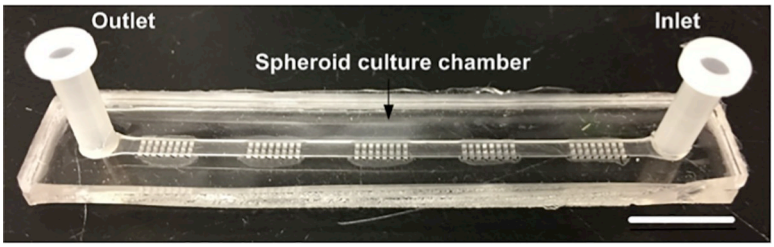

Fig 2. Design of PDMS microfluidic device developed for the culture of 3D spheroids and drug testing. Each chip is comprised of five sections of 24 wells, containing 120 wells. Each well has a dimension of 500×500×500 μm^3. The scale bar is 1 cm.

https://doi.org/10.1371/journal.pone.0244549.g002

inverted and replaced on the base of the plate containing sterile PBS for humidification and the plate was put in the incubator with the droplets hanging. Spheroids were allowed to grow for up to 6 days. For the microfluidic method, each device contained 120 spheroid culture chambers, with one inlet and one outlet (Fig 2, see fabrication section below). A cell suspension of 1 x 10^6 cells in 1 mL of complete OSE medium was used. The device was seeded with 100 μL of this suspension in the inlet, and the same amount of medium was removed from the outlet. This process was repeated by seeding in the outlet and removing medium from the inlet and performed five times in each direction (total 10 times, using all of the 1 x 10^6 cells) to allow uniform distribution of cells across the wells. Spheroids were allowed to form over 48 hours. Finally, spheroids were also prepared using 96-well round-bottom ULA plates (Corning 4515). Wells were seeded with 2000 cells in 100 μL of cooled complete OSE medium with or without 2% Matrigel (BD, Bioscience, Canada). This was done for each cell line and condition. Spheroids were allowed to form over 48 hours.

Microfluidic device fabrication

The PDMS microfluidic device used in this work is a modification of a previously described device [35]. It was made of PDMS and used the basic principle of gravity trapping [34, 41, 48]. The device layout was developed using CATIA (Dassault Systèmes, France) and the mold was carved out of polymethyl methacrylate. Using this mold, our device was made of two bonded layers of PDMS (Fig 2); 1) the bottom later contains five segments of spheroid culture chambers, each of which contains 24 wells of 500μm x 500μm x 500μm, and 2) the top layer contains a straight channel with a height of 500μm covering the entirety of the spheroid culture chambers with 3 mm holes for the inlet and outlet at the ends of the straight channel. The device was bonded using an upright microscope to align the layers after 30 sec of atmospheric plasma surface treatment. After bonding, the device was put in an oven at 80˚ C for two hours. The dimension of the device was 7.5 cm long x 1 cm wide with of 120 spheroid culture chambers (5 blocks of 24 chambers each). Nine devices could be culture at a time in an incubator using a simple pipet tip box. Prior to use, the devices were treated with 10 mg/ml Pluronic (Sigma-Aldrich, St Louis, USA) as previously described [48], to make the PDMS surface less adherent to cells. This treatment also prevents chemo-absorption by the PDMS [49].

Carboplatin treatment

Previously, we have shown that the carboplatin IC_{50} for spheroids from a specific EOC cell line (TOV112D) is approximately 10x the corresponding monolayer IC_{50} value [41]. Therefore, as the most resistant cell line in this study has an IC_{50} of 30μM (Table 1), we treated the spheroids formed in the PDMS-based microfluidic systems and in the ULA plates with 300 μM

carboplatin. Moreover, in our earlier pilot studies using concentrations 10 times lower (30 μM) and 10 times higher (3000 μM), no differential results among the cell lines were observed, as they all survived at the lower dose and all died at the higher. Interestingly, the 300 μM carboplatin concentration is similar to that found in the plasma of ovarian cancer patients undergoing chemotherapy [48]. Spheroids formed 48 hours after cell seeding were treated with fresh medium (controls) or fresh medium containing 300 μM carboplatin (Hospira Healthcare Corporation) for a period of 48 hours. Carboplatin treatment was also performed on monolayer cultures prepared with 5,000 cells/well of each cell line seeded into 6-well plates. Consistent with the method for spheroids, 48 hours after inoculation, the cultures were treated with fresh medium (controls) or fresh medium containing 300 μM carboplatin and cultures were incubated for 48 hours. After treatment samples were immediately used in subsequent analyses.

Microscopy and imaging

Microscopy images were taken using an inverted microscope (Nikon TS100) at 10X or 4X magnification two and four days after seeding as well as 48 hours after treatment prior to flow cytometry analysis. PDMS microfluidic devices were put into a 100 mm petri dish for imaging purposes to maintain sterile conditions. Size estimation was done using ImageJ software (Version 1.49, National Institute of Health, Bethesda, MD).

Flow cytometry analysis

After carboplatin treatment, monolayer cells from each well of the 6-well plates were harvested by trypsin-EDTA (0.05%) as a single cell suspension. For the spheroids treated in the ULA plates, 10 were collected, pooled and dissociated with trypsin-EDTA (0.05%) for 5 minutes to obtain single-cell suspensions. For those treated in the PDMS-based microfluidic devices, 48 were pooled and dissociated as above. Cells were then labelled with Annexin-V (3:100 dilution) and 7-Amino-ActinomycinD (7-AAD, 5:100 dilution) to detect apoptotic and dead cells, respectively (PE Annexin V apoptosis Detection Kit I, BD Biosciences). After a 15-minute incubation at RT (25˚C) in the dark, the stained cells were analyzed by flow cytometry (LSR-Fortessa, BD Biosciences), within 2 hours of staining. The data collected from each acquisition was analyzed using the FlowJo software (FlowJo, LLC, Ashland, USA). After excluding cell debris, viable cells were selected based on the absence of 7-AAD and/or Annexin-V markers (see example on S1 Fig).

Statistical analysis

Values are expressed as the mean ± SEM (standard error of the mean), derived from at least three independent experiments. Single comparisons between two groups were determined by Student's t-test (paired, two-tailed). Comparisons between multiple groups were determined by Tukey ANOVA multi comparison test. P values < 0.05 were considered significant. All statistical analyses were done using GraphPad Prism 6 software (GraphPad Software Inc., San Diego, CA).

Results

Comparison of spheroid formation using different methods

In order to compare carboplatin sensitivity of different EOC cell lines in 2D monolayers and in 3D spheroids obtained by different methods, we first evaluated the efficiency of each 3D technique (hanging-droplets, ULA plates, and PDMS-based microfluidic chips) to form

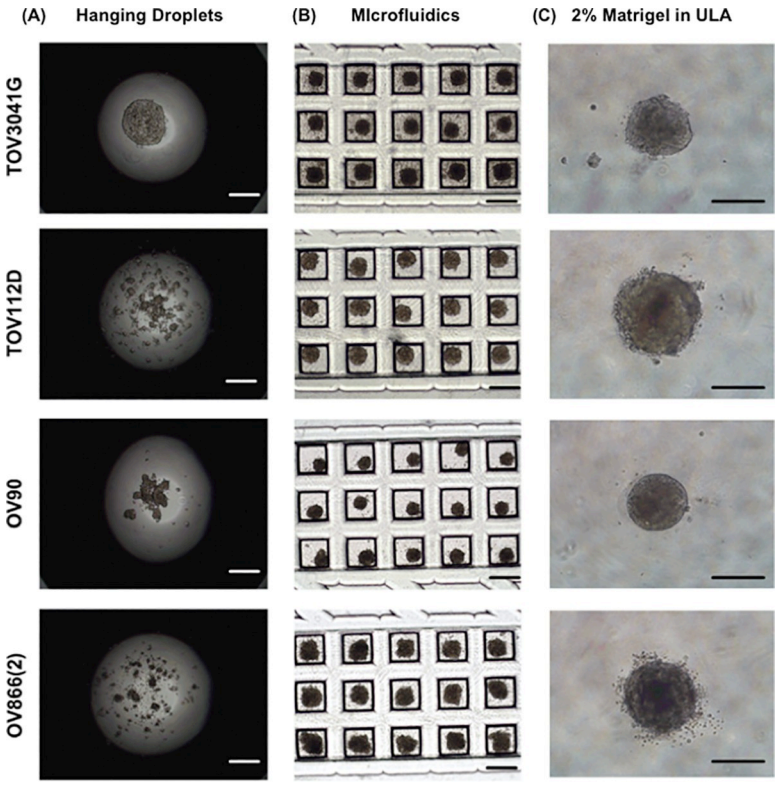

Fig 3. Capacity of EOC cell lines to form spheroids in three different culture conditions. Representative microscopic bright field images of TOV3041G, TOV112D, OV90 and OV866(2) cells cultured 48 hours in hanging droplets (A), within the custom PDMS-based microfluidic chips, (B) and in 96-well round-bottom ULA plates with 2% Matrigel (C). The scale bar is 500 μm.

https://doi.org/10.1371/journal.pone.0244549.g003

spheroids using four EOC cell lines [TOV3041G, TOV112D, OV90 and OV866(2)]. Fig 3A shows the hanging-droplet cultures at day 2 with the four EOC cell lines. Only TOV3041G formed spheroids within 48 hours. Careful observation showed that, at this time point, TOV112D and OV90 had started to form multiple smaller spheroids. However, OV866(2) had not formed spheroids at all. Culturing the same cell lines up to day 4 and day 6, we observed that the smaller spheroids of TOV112D and OV90 had fused together to form larger spheroids (S2 Fig). However, OV866(2) did not show any sign of spheroid formation. Fig 3B shows bright field images of 3D cultures at day 2 using the PDMS-based microfluidic device. All cell lines formed spheroids in the microfluidic device within 48 hours. Fig 3C shows the bright field images of Matrigel-assisted spheroids using ULA wells at 48 hours. Again, all the cell lines formed spheroid within 48 hours. However, less compact spheroids were obtained when EOC cell lines were grown in the ULA plates in the absence of Matrigel (S3 Fig). Therefore, carboplatin sensitivity was evaluated in 3D spheroids formed in the PDMS microfluidic device and the Matrigel-assisted ULA plate since the latter is widely used for drug sensitivity assays [11, 18, 19, 45, 50].

Carboplatin sensitivity of EOC cell line spheroids obtained by two different methods

Sensitivity of the spheroids was evaluated at a concentration of 300 μM carboplatin, a concentration similar to that found in the plasma of ovarian cancer patients undergoing chemotherapy [48]. This concentration is in range of what has been used in other studies (100 μM,

330 μM) to evaluate platinum sensitivity of ovarian cancer spheroids [18, 46]. It is also 10 times higher than the 2D IC_{50} (by clonogenic assay) of the most resistant cell lines OV90 and OV866(2) (see Table 1). Then, the effect of carboplatin on our EOC cell lines was evaluated by measuring the size of the spheroids, as is commonly used in the literature [18, 19, 45, 51], and by measuring live/apoptotic/dead cells by flow cytometry using Annexin V/7-AAD staining of the dissociated spheroids. For the spheroids grown in the PDMS-based microfluidic chips, we observed a significant decrease in the percentage of live cells following treatment with 300 μM carboplatin for the OV90 and OV866(2) spheroids, but not for the TOV3041G and TOV112D cells, the latter being the most resistant in this assay (Fig 4B). However, no significant decrease

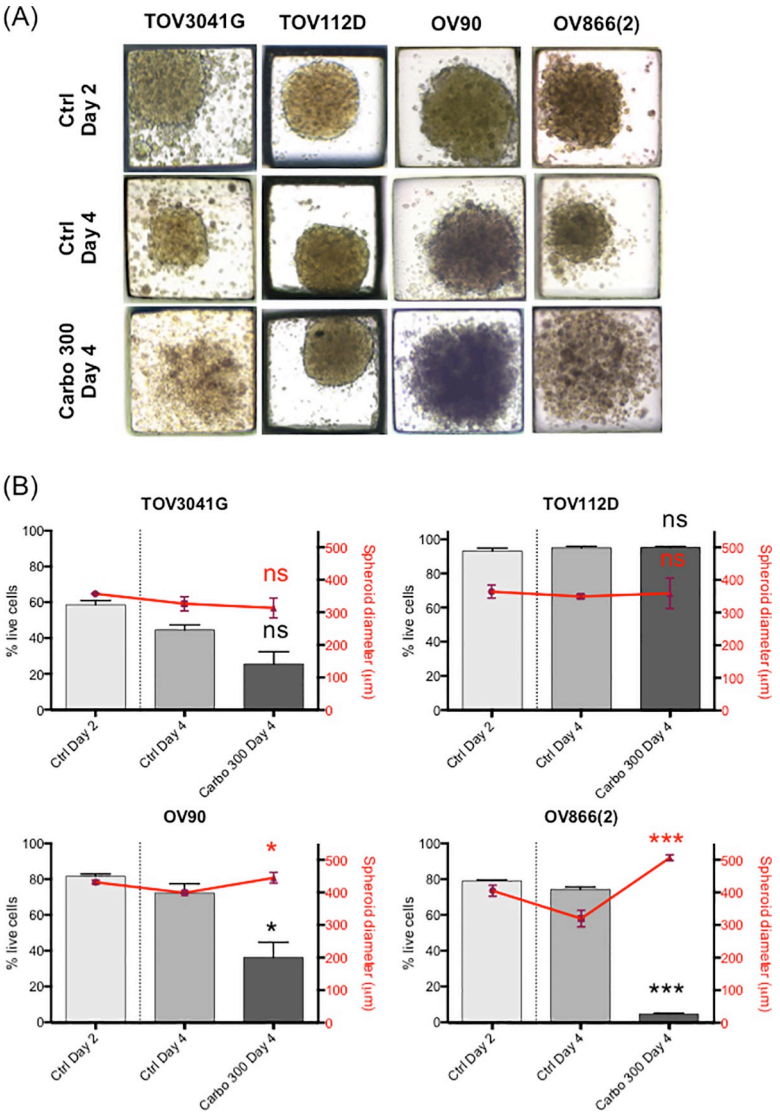

Fig 4. Carboplatin response of EOC spheroids cultured in PDMS microfluidic devices. 3D spheroids of four EOC cell lines [TOV3041G, TOV112D, OV90, OV866(2)] were formed and cultured in microfluidic devices for 2 and 4 days (Ctrl Day 2 and Ctrl Day 4) or treated at day 2 with 300 μM of carboplatin and assessed at day 4 (Carbo 300 Day 4). A) Representative microscopic bright field images at 10X magnification. B) Comparison of carboplatin treatment on EOC cell survival (grey bars) and spheroid diameters (red points). 48 spheroids were analyzed (in duplicate) from each set of experiment readouts. Error bars indicate the standard errors of the mean (SEM) of three independent experiments. Statistical analyses: Ctrl Day 4 vs Carbo 300 Day 4, * $p<0.05$; *** $p<0.0005$; ns, non-significant (Student's t-test).

https://doi.org/10.1371/journal.pone.0244549.g004

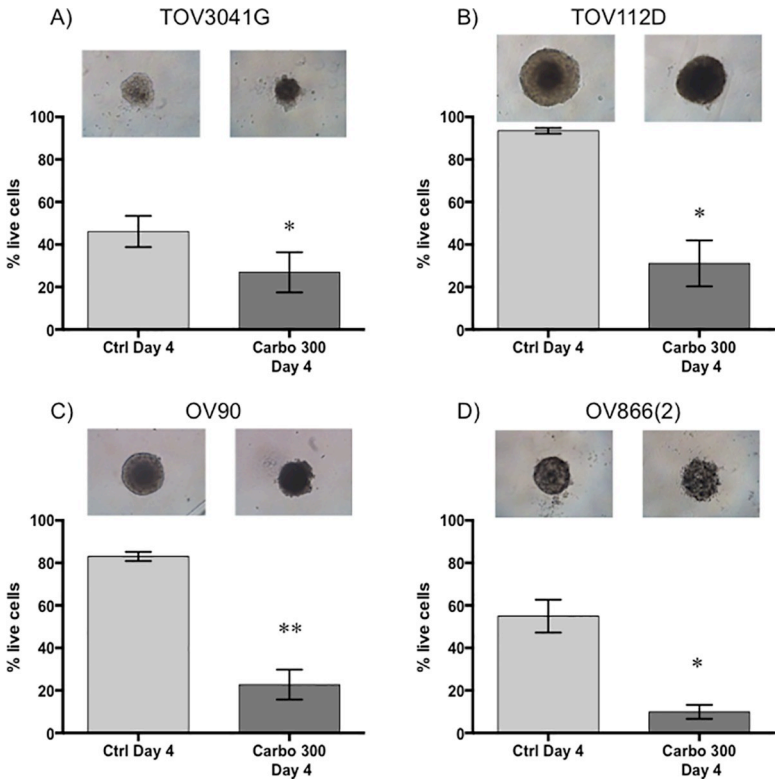

Fig 5. Carboplatin response of EOC spheroids cultured with 2% matrigel in ultra-low attachment wells. 3D spheroids of TOV3041G (A), TOV112D (B), OV90 (C) and OV866(2) (D) were formed and cultured in concave-bottom ULA plates in the presence of 2% Matrigel for 4 days (Ctrl Day 4) or treated at day 2 with 300 μM of carboplatin and assessed at day 4 (Carbo 300 Day 4). Top panels are representative microscopic bright field images of each condition. Bar graphs represent cell survival analysed by flow cytometry of control (light grey) and treated (dark grey) spheroids. Data are shown as the mean ± SEM of three independent experiments. * $p<0.05$; ** $p<0.005$ (Student's t-test).

https://doi.org/10.1371/journal.pone.0244549.g005

in the size of spheroids was observed, and on the contrary, sizes of the OV90 and OV866(2) spheroids were significantly increased, likely due to spheroid disaggregation (Fig 4A and 4B). For spheroids grown in the Matrigel-assisted ULA plates, our results showed that all four cell lines presented decreased viability after incubation with 300 μM carboplatin, including TOV112D, as assessed by Annexin V/7-AAD staining and flow cytometry, but we did not notice a change in size when visually inspecting these spheroids (Fig 5 inserts). In the Matrigel-assisted ULA plates the highest resistance to carboplatin was observed in the TOV3041G cell line. Of note, sizes of non-treated spheroids were less than 500 μm in diameter in days 2 and 4 in both methods (Figs 3–5), which is important to avoid extensive internal necrotic core.

Comparative carboplatin response of 3D spheroids with that of 2D monolayers

The carboplatin sensitivity of cell lines in 2D culture was originally obtained using the clonogenic assay (Table 1), where cells are plated at a low dilution in order to obtain colonies from single cells. However, in our 3D spheroid assays (both methods), a large number of cells are used to form the spheroids and carboplatin sensitivity is determined by the percentage of residual live cells. In order to approximate analysis methods used for the 2D and 3D drug sensitivity assays, we treated cell monolayers at 80% confluence with carboplatin (300 μM), and

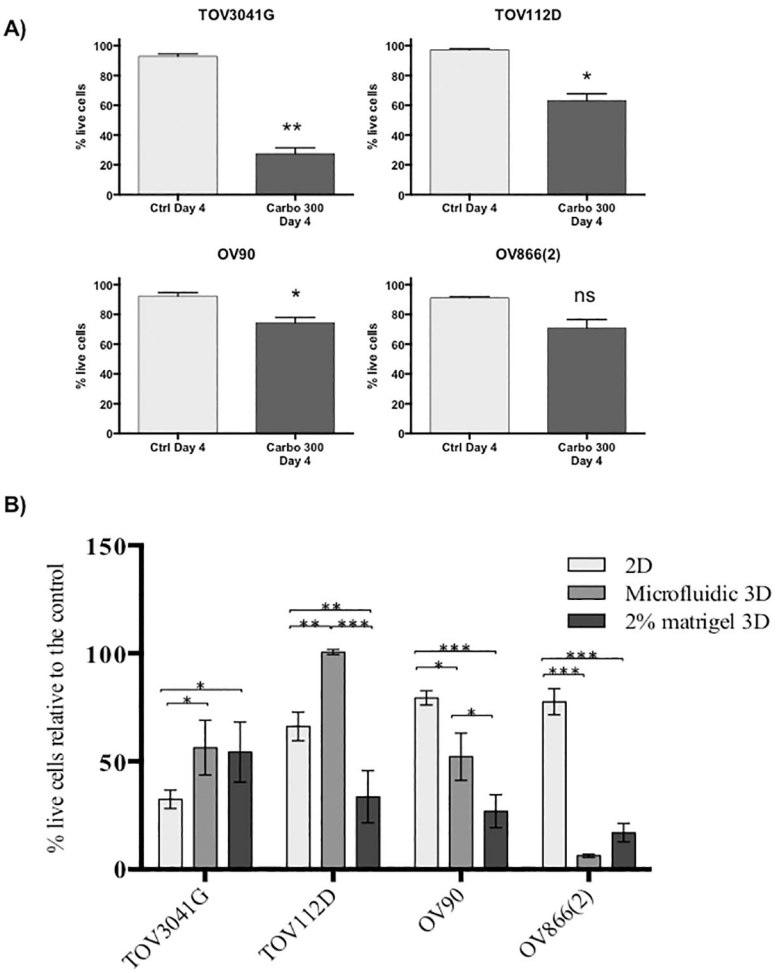

Fig 6. Comparison of carboplatin response between 2D-monolayers and two different 3D spheroid models. A) TOV3041G, TOV112D, OV90 and OV866(2) were culture as 2D monolayers for 4 days without treatment (Ctrl Day 4) or treated at day 2 with 300 μM of carboplatin and assessed at day 4 (Carbo 300 Day 4). Bar graphs represent cell survival analysed by flow cytometry of control (light grey) and treated (dark grey). Data are shown as the mean ± SEM of three independent experiments * $p<0.05$; ** $p<0.005$; ns, non-significant (Student's t-test) **B)** 2D-monolayer carboplatin sensitivity was compared to that of 3D spheroid cultures. Each treatment response was normalized relative to the percentage of live cells in comparison to the appropriate control. * p-value <0.05; ** p-value <0.005; *** p-value <0.0005; Turkey ANOVA multi comparison test of three independent experiments.

https://doi.org/10.1371/journal.pone.0244549.g006

evaluated cell viability by flow cytometry as for the spheroids. Sensitivity of 2D monolayers (Fig 6A) corresponded proportionately with that of the clonogenic assays where TOV3041G was the most sensitive and OV90 and OV866(2) the most resistant (Table 1).

When comparing the percentage of live cells by flow cytometry (normalized to controls) in the three methods tested, i.e. monolayer, spheroids from PDMS-based microfluidic devices and Matrigel-assisted spheroids, we observed that the spheroids of TOV3041G were significantly more resistant to carboplatin than in monolayer culture, and that the spheroids of OV90 and OV866(2) were significantly more sensitive than their respective monolayer cultures. This was independent of the spheroid formation method used (Fig 6B). However, when comparing both 3D cultures, OV90 spheroids formed in the microfluidic devices were significantly more resistant than those obtained using Matrigel-assisted ULA plates. However, both spheroid models were significantly more sensitive than the monolayer cultures. In contrast,

spheroids of the TOV112D cell line formed in the microfluidic device were more resistant than the monolayer culture but were more sensitive when formed by the Matrigel-assisted technique. Table 2 summarizes this comparative study, in which a cell line ranking #1 has lower viability (more sensitivity) than the cell line ranking as #2, and this approach was further applied to determine rank order. When cell lines have similar percentage of cell survival, the same ranking is given to both of them. This classification shows a clear inversion of sensitivity from 2D to 3D for two of the four cell lines studied, in which the most sensitive becomes resistant to carboplatin (TOV3041G) and the most resistant becomes the most sensitive [OV866(2)].

Discussion

In recent years, 3D cell culture models such as multi-cellular spheroids have become more widely used as pre-clinical models and are expected to bridge the gap between 2D and animal models. In the particular case of ovarian cancer, 3D spheroids are clinically relevant models since in advanced disease EOC cells can spread to the peritoneum as aggregates/spheroids [52, 53]. In the literature, several EOC cell lines have been studied by different spheroid generating methods, including hanging-droplets [16, 22, 27–29, 41, 54, 55], biomimetic hydrogels [23], plastic wells coated with matrix scaffolds [20, 46, 56], and more recently by microfluidics [33, 34, 37, 38, 42, 44] and commercially available round-bottom ULA plates [18, 45, 50, 57]. In the present study we first compared the ability of four EOC cell lines to form spheroids using these ULA 96-well plates (in the absence or presence of Matrigel) with that of hanging-droplets and PDMS-based microfluidic chips. For the latter, we used a recently developed [34, 37, 38] PDMS microfluidic device with a capacity of 120 spheroids per device. We showed that both Matrigel-assisted ULA plates and simple well-based PDMS microfluidic devices were the most robust and efficient methods to form spheroids. However, our microfluidic devices have the advantage of using much smaller volumes of media or drug, which is desirable when working with expensive compounds or extensive drug screenings.

We evaluated the carboplatin response of EOC cell lines grown as spheroids using these two methods and compared these to the respective monolayer cultures. Spheroid size is widely used as a measure of drug response in several studies, including those with EOC cells [18, 19, 45, 51], where decreased spheroid size has been interpreted as reflecting cell death [19]. In contrast, our results show that, independent of the method of spheroid formation used, no decrease in spheroid volume was observed. However, a significant increase in spheroid volume was observed for two cell lines [OV90 and OV866(2)] when using PDMS-based microfluidic devices, likely reflecting spheroid disaggregation due to cell death. Our findings indicate that spheroid size is not appropriate to be used as a measurement of carboplatin response, at least when using a short incubation time (like 48h of this study), as cell dissociation/disaggregation due to cell death/apoptosis would increase spheroid size. Therefore, the response of the spheroids and monolayers to the drug was also assessed by the broadly accepted method of flow cytometry through the analysis of apoptosis (Annexin V) and cell death (7-AAD). We

Table 2. Relative carboplatin sensitivity of four EOC cell lines in three different culture conditions.

Cell line	2D culture model	3D culture model	
		PDMS Microfluidic devices	Ultra-low attachment wells and 2% Matrigel
TOV3041G	1	2	**3**
TOV112D	2	**3**	2
OV90	**3**	2	2
OV866(2)	**3**	1	1

https://doi.org/10.1371/journal.pone.0244549.t002

observed decreased cell survival of spheroids after carboplatin treatment, with the highest level of cell death being observed in the two cell lines that showed increased spheroid volumes. Strikingly, in three of the four cell lines studied, the 3D sensitivity (independent of the spheroid formation method used) was inverted when compared with the corresponding 2D test, where two cell lines [OV90 and OV866(2)] classified as resistant in 2D cultures became sensitive in 3D models, and one sensitive cell line (TOV3041G) in 2D culture showed resistance in the 3D model. The latter result is more consistent with the literature where 3D spheroids are more resistant than 2D cultures [11, 18, 34, 41, 46, 58]. Although the exact signaling mechanism implicated in this resistance is still unclear, reports have attributed it to decreased compound access, reduced sensitivity in response to hypoxia, cells cycling more slowly, cell-cell contact influence, and an increased EMT phenotype [11, 12, 58].

In a recent report [18], a comparative analysis of cisplatin response of monolayer cultures and 3D spheroids of 16 EOC cell lines showed that the majority of the spheroids (13/16) were more resistant to cisplatin than the respective 2D cultures (much as we have observed with the TOV3041G cell line), whereas two cell lines were equally sensitive and one showed higher sensitivity in 3D spheroids than 2D monolayers, the latter similar to what we observed in two of our cell lines [OV9 and OV866(2)]. Another study using 11 EOC cell lines showed increased cisplatin resistance of 3D spheroids in seven cell lines, with no change for the other four [46]. It is possible too that the read-out methods used in these studies have underestimated spheroids cell death when compared to ours. In these articles, platinum sensitivity of ovarian cancer cell lines cultured as 3D spheroids have been mainly evaluated by metabolic assay (since it is a more high-throughput assay) that would overestimate cell survival, as early apoptotic or senescent cells are still metabolically active. We think that the cell death/apoptosis/cell viability FACS method used in our work, although less high-throughput, would more accurately estimate cell survival after carboplatin treatment in 3D spheroids. Nevertheless, all together, these findings imply that the assumption that spheroids are more resistant to chemotherapy than the monolayer cultures is not always accurate and may influence the choice of EOC models used to study chemoresistance. Previous publications have attempted to correlate molecular features (i.e. epithelial and mesenchymal protein biomarkers) with platinum sensitivity of ovarian cancer cell lines grown as 2D *vs* 3D [18, 46]. Based in these results, it is unlikely that these factors play a role in the sensitivity inversion of our cell lines.

When comparing the two spheroid models, we generally obtained similar carboplatin responses, except for the TOV112D cell line. Spheroids of this cell line were more resistant than the monolayer when assayed using the PDMS-based microfluidic device, but more sensitive in the Matrigel-assisted ULA plates. It is possible that this cell line is more affected by the Matrigel presence than the others. It is known that ECM components, like Matrigel, can affect drug responses [11]. Although we treated our PDMS devices with pluronic to prevent cell adherence and chemo-absorption [49], performing 3D assays in both PDMS chips and conventional plates enabled us to rule out the well-known absorption of drugs by the hydrophobic porous matrix of the PDMS as a significant cause for this discrepancy [59]. While the absorbed concentration has not been directly controlled, our results (Fig 6B) do not show a systematic increase in resistance in the PDMS devices as would be suggested if the cells are experiencing an effectively lower concentration due to material absorption. Rather, resistance is slightly lower in one cell line [OV866(2)] and significantly higher in another one (TOV112D). Regarding the latter, it is possible that this cell line is more affected by components of the ECM that might influence drug efficacy. Matrigel is a mixture of different ECM components that has high variability issues due to batch effect [60], making it difficult to thoroughly investigate the role of this ECM mimic in the 3D chemosensitivity of this cell line. Therefore, because PDMS-based microfluidic devices were fast, reliable and high-throughput for the analyses of 3D

spheroids, and because they used very small media/drug volumes, they make an interesting alternative choice for drug screening either in pharmaceutical research or in clinical settings. In a very recent report, 3D spheroids from tumor tissue of ovarian cancer patients were obtained using the round-bottom ULA plates (without Matrigel) [57]. When compared to clinical outcome, response of these patient-derived 3D spheroids to chemotherapeutic drugs, including the standard of care carboplatin-paclitaxel combination therapy, showed concordance in 89% of the cases (39 of 44) [57]. However, spheroids of different sizes, shapes and compactions were observed from sample to sample and a high number of replicates were needed. The PDMS microfluidic device described here may overcome this technical difficulty by providing a large number of uniform spheroids to be tested for drug response using less patient sample, suggesting that it could easily be incorporated into a clinic setting or used for drug development in the future.

Although descriptive, the present work aims to emit a clear warning that there is no strong tendency of EOC cells to become more resistant in 3D than in 2D, and that spheroid size is an inefficient predictor of cell response as size variation can be both a change of cell number or a change in tissue compactness.

Conclusion

In drug discovery, the choice of an appropriate *in vitro* pre-clinical model can have a major influence on correctly predicting drug response in human clinical trials. Here, we evaluated carboplatin sensitivity of four epithelial ovarian cancer cell lines using both 2D and 3D *in vitro* models and tested different spheroid forming methods. Channel-based spheroid forming chips held several advantages over commercially available ultra-low attachment plates or the hanging droplet method. Irrespective of the spheroid forming method used, some striking carboplatin sensitivity inversions were noted within a given cell line when 2D and 3D results were compared. Overall, the present study highlights the challenges of *in vitro* models and discusses the different facets of 2D and 3D *in vitro* drug testing.

Supporting information

S1 Fig. 7-AAD and Annexin-V flow cytometry analysis. Graphs represent an example of flow cytometry analysis of spheroids treated with 300 μM carboplatin and its respective control. After excluding cell debris, viable cells were selected based on the absence of 7-AAD and/or Annexin-V markers (red square). Apoptotic and/or dead cells are shown in the other quadrants.
(TIF)

S2 Fig. Spheroid formation using hanging drops with different EOC cell lines. (A) Bright field images at day 4. (B) Bright field images at day 6. Scale bar, 500 μm.
(TIF)

S3 Fig. Spheroid formation using ULA round-bottom wells (without Matrigel) with different EOC cell lines. Bright field images at day 2. Note that TOV112D cells in these conditions form multiple spheroids of smaller size. Scale bar, 300 μm.
(TIF)

Acknowledgments

We acknowledge Jennifer Kendall-Dupont for technical assistance. We thank the Institut du cancer de Montréal (ICM) Cytometry and Microscopy Core Facilities.

Author Contributions

Conceptualization: Bishnubrata Patra, Euridice Carmona, Anne-Marie Mes-Masson, Thomas Gervais.

Data curation: Benjamin Péant.

Formal analysis: Bishnubrata Patra, Muhammad Abdul Lateef, Hubert Fleury, Benjamin Péant.

Funding acquisition: Diane Provencher, Anne-Marie Mes-Masson, Thomas Gervais.

Investigation: Bishnubrata Patra, Euridice Carmona.

Methodology: Bishnubrata Patra, Muhammad Abdul Lateef, Hubert Fleury.

Project administration: Euridice Carmona.

Supervision: Euridice Carmona, Benjamin Péant, Anne-Marie Mes-Masson, Thomas Gervais.

Validation: Muhammad Abdul Lateef.

Visualization: Bishnubrata Patra, Melica Nourmoussavi Brodeur, Benjamin Péant.

Writing – original draft: Bishnubrata Patra, Muhammad Abdul Lateef, Melica Nourmoussavi Brodeur, Euridice Carmona.

Writing – review & editing: Bishnubrata Patra, Muhammad Abdul Lateef, Melica Nourmoussavi Brodeur, Hubert Fleury, Euridice Carmona, Benjamin Péant, Diane Provencher, Anne-Marie Mes-Masson, Thomas Gervais.

References

1. Siegel RL, Miller KD, Jemal A. Cancer statistics, 2019. CA Cancer J Clin. 2019; 69(1):7–34. https://doi.org/10.3322/caac.21551 PMID: 30620402
2. Lheureux S, Gourley C, Vergote I, Oza AM. Epithelial ovarian cancer. Lancet. 2019; 393(10177):1240–53. https://doi.org/10.1016/S0140-6736(18)32552-2 PMID: 30910306
3. Coleman RL, Monk BJ, Sood AK, Herzog TJ. Latest research and treatment of advanced-stage epithelial ovarian cancer. Nature reviews Clinical oncology. 2013; 10(4):211–24. https://doi.org/10.1038/nrclinonc.2013.5 PMID: 23381004
4. Wilson MK, Pujade-Lauraine E, Aoki D, Mirza MR, Lorusso D, Oza AM, et al. Fifth Ovarian Cancer Consensus Conference of the Gynecologic Cancer InterGroup: recurrent disease. Annals of oncology: official journal of the European Society for Medical Oncology. 2017; 28(4):727–32.
5. Imamura Y, Mukohara T, Shimono Y, Funakoshi Y, Chayahara N, Toyoda M, et al. Comparison of 2D- and 3D-culture models as drug-testing platforms in breast cancer. Oncol Rep. 2015; 33(4):1837–43. https://doi.org/10.3892/or.2015.3767 PMID: 25634491
6. Johnson JI, Decker S, Zaharevitz D, Rubinstein LV, Venditti JM, Schepartz S, et al. Relationships between drug activity in NCI preclinical in vitro and in vivo models and early clinical trials. British journal of cancer. 2001; 84(10):1424–31. https://doi.org/10.1054/bjoc.2001.1796 PMID: 11355958
7. Phillips RM, Bibby MC, Double JA. A critical appraisal of the predictive value of in vitro chemosensitivity assays. Journal of the National Cancer Institute. 1990; 82(18):1457–68. https://doi.org/10.1093/jnci/82.18.1457 PMID: 2202838
8. Riedl A, Schlederer M, Pudelko K, Stadler M, Walter S, Unterleuthner D, et al. Comparison of cancer cells in 2D vs 3D culture reveals differences in AKT-mTOR-S6K signaling and drug responses. J Cell Sci. 2017; 130(1):203–18. https://doi.org/10.1242/jcs.188102 PMID: 27663511
9. Elliott NT, Yuan F. A review of three-dimensional in vitro tissue models for drug discovery and transport studies. Journal of pharmaceutical sciences. 2011; 100(1):59–74. https://doi.org/10.1002/jps.22257 PMID: 20533556
10. Nyga A, Cheema U, Loizidou M. 3D tumour models: novel in vitro approaches to cancer studies. Journal of cell communication and signaling. 2011; 5(3):239–48. https://doi.org/10.1007/s12079-011-0132-4 PMID: 21499821

11. Xu X, Farach-Carson MC, Jia X. Three-dimensional in vitro tumor models for cancer research and drug evaluation. Biotechnology advances. 2014; 32(7):1256–68. https://doi.org/10.1016/j.biotechadv.2014.07.009 PMID: 25116894

12. Hoarau-Vechot J, Rafii A, Touboul C, Pasquier J. Halfway between 2D and Animal Models: Are 3D Cultures the Ideal Tool to Study Cancer-Microenvironment Interactions? International journal of molecular sciences. 2018; 19(1). https://doi.org/10.3390/ijms19010181 PMID: 29346265

13. Frey O, Misun PM, Fluri DA, Hengstler JG, Hierlemann A. Reconfigurable microfluidic hanging drop network for multi-tissue interaction and analysis. Nature communications. 2014; 5:4250. https://doi.org/10.1038/ncomms5250 PMID: 24977495

14. Pampaloni F, Reynaud EG, Stelzer EH. The third dimension bridges the gap between cell culture and live tissue. Nature reviews Molecular cell biology. 2007; 8(10):839–45. https://doi.org/10.1038/nrm2236 PMID: 17684528

15. Tung YC, Hsiao AY, Allen SG, Torisawa YS, Ho M, Takayama S. High-throughput 3D spheroid culture and drug testing using a 384 hanging drop array. Analyst. 2011; 136(3):473–8. https://doi.org/10.1039/c0an00609b PMID: 20967331

16. Zietarska M, Maugard CM, Filali-Mouhim A, Alam-Fahmy M, Tonin PN, Provencher DM, et al. Molecular description of a 3D in vitro model for the study of epithelial ovarian cancer (EOC). Molecular carcinogenesis. 2007; 46(10):872–85. https://doi.org/10.1002/mc.20315 PMID: 17455221

17. Castaneda F, Kinne RK. Short exposure to millimolar concentrations of ethanol induces apoptotic cell death in multicellular HepG2 spheroids. Journal of cancer research and clinical oncology. 2000; 126(6):305–10. https://doi.org/10.1007/s004320050348 PMID: 10870639

18. Heredia-Soto V, Redondo A, Berjon A, Miguel-Martin M, Diaz E, Crespo R, et al. High-throughput 3-dimensional culture of epithelial ovarian cancer cells as preclinical model of disease. Oncotarget. 2018; 9(31):21893–903. https://doi.org/10.18632/oncotarget.25098 PMID: 29774110

19. Vinci M, Gowan S, Boxall F, Patterson L, Zimmermann M, Court W, et al. Advances in establishment and analysis of three-dimensional tumor spheroid-based functional assays for target validation and drug evaluation. BMC biology. 2012; 10:29. https://doi.org/10.1186/1741-7007-10-29 PMID: 22439642

20. Chen J, Wang J, Chen D, Yang J, Yang C, Zhang Y, et al. Evaluation of characteristics of CD44+CD117+ ovarian cancer stem cells in three dimensional basement membrane extract scaffold versus two dimensional monocultures. BMC cell biology. 2013; 14:7. https://doi.org/10.1186/1471-2121-14-7 PMID: 23368632

21. Chen MW, Yang ST, Chien MH, Hua KT, Wu CJ, Hsiao SM, et al. The STAT3-miRNA-92-Wnt Signaling Pathway Regulates Spheroid Formation and Malignant Progression in Ovarian Cancer. Cancer research. 2017; 77(8):1955–67. https://doi.org/10.1158/0008-5472.CAN-16-1115 PMID: 28209618

22. Dong Y, Stephens C, Walpole C, Swedberg JE, Boyle GM, Parsons PG, et al. Paclitaxel resistance and multicellular spheroid formation are induced by kallikrein-related peptidase 4 in serous ovarian cancer cells in an ascites mimicking microenvironment. PloS one. 2013; 8(2):e57056. https://doi.org/10.1371/journal.pone.0057056 PMID: 23451143

23. Loessner D, Stok KS, Lutolf MP, Hutmacher DW, Clements JA, Rizzi SC. Bioengineered 3D platform to explore cell-ECM interactions and drug resistance of epithelial ovarian cancer cells. Biomaterials. 2010; 31(32):8494–506. https://doi.org/10.1016/j.biomaterials.2010.07.064 PMID: 20709389

24. Masiello T, Dhall A, Hemachandra LPM, Tokranova N, Melendez JA, Castracane J. A Dynamic Culture Method to Produce Ovarian Cancer Spheroids under Physiologically-Relevant Shear Stress. Cells. 2018; 7(12). https://doi.org/10.3390/cells7120277 PMID: 30572633

25. Nunes AS, Barros AS, Costa EC, Moreira AF, Correia IJ. 3D tumor spheroids as in vitro models to mimic in vivo human solid tumors resistance to therapeutic drugs. Biotechnology and bioengineering. 2019; 116(1):206–26. https://doi.org/10.1002/bit.26845 PMID: 30367820

26. Rafehi S, Ramos Valdes Y, Bertrand M, McGee J, Prefontaine M, Sugimoto A, et al. TGFbeta signaling regulates epithelial-mesenchymal plasticity in ovarian cancer ascites-derived spheroids. Endocrine-related cancer. 2016; 23(3):147–59. https://doi.org/10.1530/ERC-15-0383 PMID: 26647384

27. Fleury H, Communal L, Carmona E, Portelance L, Arcand SL, Rahimi K, et al. Novel high-grade serous epithelial ovarian cancer cell lines that reflect the molecular diversity of both the sporadic and hereditary disease. Genes Cancer. 2015; 6(9–10):378–98. https://doi.org/10.18632/genesandcancer.76 PMID: 26622941

28. Letourneau IJ, Quinn MC, Wang LL, Portelance L, Caceres KY, Cyr L, et al. Derivation and characterization of matched cell lines from primary and recurrent serous ovarian cancer. BMC Cancer. 2012; 12:379. https://doi.org/10.1186/1471-2407-12-379 PMID: 22931248

29. Ouellet V, Zietarska M, Portelance L, Lafontaine J, Madore J, Puiffe ML, et al. Characterization of three new serous epithelial ovarian cancer cell lines. BMC Cancer. 2008; 8:152. https://doi.org/10.1186/1471-2407-8-152 PMID: 18507860

30. Gupta N, Liu JR, Patel B, Solomon DE, Vaidya B, Gupta V. Microfluidics-based 3D cell culture models: Utility in novel drug discovery and delivery research. Bioeng Transl Med. 2016; 1(1):63–81. https://doi.org/10.1002/btm2.10013 PMID: 29313007

31. Joshi P, Lee MY. High Content Imaging (HCI) on Miniaturized Three-Dimensional (3D) Cell Cultures. Biosensors (Basel). 2015; 5(4):768–90. https://doi.org/10.3390/bios5040768 PMID: 26694477

32. Fridman R, Benton G, Aranoutova I, Kleinman HK, Bonfil RD. Increased initiation and growth of tumor cell lines, cancer stem cells and biopsy material in mice using basement membrane matrix protein (Cultrex or Matrigel) co-injection. Nature protocols. 2012; 7(6):1138–44. https://doi.org/10.1038/nprot.2012.053 PMID: 22596226

33. Marimuthu M, Rousset N, St-Georges-Robillard A, Lateef MA, Ferland M, Mes-Masson AM, et al. Multi-size spheroid formation using microfluidic funnels. Lab Chip. 2018; 18(2):304–14. https://doi.org/10.1039/c7lc00970d PMID: 29211088

34. Patra B, Lafontaine J, Bavoux M, Zerouali K, Glory A, Ahanj M, et al. On-chip combined radiotherapy and chemotherapy testing on soft-tissue sarcoma spheroids to study cell death using flow cytometry and clonogenic assay. Sci Rep. 2019; 9(1):2214. https://doi.org/10.1038/s41598-019-38666-9 PMID: 30778138

35. Patra B, Peng CC, Liao WH, Lee CH, Tung YC. Drug testing and flow cytometry analysis on a large number of uniform sized tumor spheroids using a microfluidic device. Sci Rep. 2016; 6:21061. https://doi.org/10.1038/srep21061 PMID: 26877244

36. Sart S, Tomasi RF, Amselem G, Baroud CN. Multiscale cytometry and regulation of 3D cell cultures on a chip. Nature communications. 2017; 8(1):469. https://doi.org/10.1038/s41467-017-00475-x PMID: 28883466

37. St-Georges-Robillard A, Cahuzac M, Peant B, Fleury H, Lateef MA, Ricard A, et al. Long-term fluorescence hyperspectral imaging of on-chip treated co-culture tumour spheroids to follow clonal evolution. Integrative biology: quantitative biosciences from nano to macro. 2019; 11(4):130–41. https://doi.org/10.1093/intbio/zyz012 PMID: 31172192

38. St-Georges-Robillard A, Masse M, Cahuzac M, Strupler M, Patra B, Orimoto AM, et al. Fluorescence hyperspectral imaging for live monitoring of multiple spheroids in microfluidic chips. Analyst. 2018; 143 (16):3829–40. https://doi.org/10.1039/c8an00536b PMID: 29999046

39. Zuchowska A, Kwapiszewska K, Chudy M, Dybko A, Brzozka Z. Studies of anticancer drug cytotoxicity based on long-term HepG2 spheroid culture in a microfluidic system. Electrophoresis. 2017; 38 (8):1206–16. https://doi.org/10.1002/elps.201600417 PMID: 28090668

40. Chen YC, Lou X, Zhang Z, Ingram P, Yoon E. High-Throughput Cancer Cell Sphere Formation for Characterizing the Efficacy of Photo Dynamic Therapy in 3D Cell Cultures. Sci Rep. 2015; 5:12175. https://doi.org/10.1038/srep12175 PMID: 26153550

41. Das T, Meunier L, Barbe L, Provencher D, Guenat O, Gervais T, et al. Empirical chemosensitivity testing in a spheroid model of ovarian cancer using a microfluidics-based multiplex platform. Biomicrofluidics. 2013; 7(1):11805. https://doi.org/10.1063/1.4774309 PMID: 24403987

42. Li SS, Ip CK, Tang MY, Sy SK, Yung S, Chan TM, et al. Modeling Ovarian Cancer Multicellular Spheroid Behavior in a Dynamic 3D Peritoneal Microdevice. Journal of visualized experiments: JoVE. 2017(120).

43. Ruppen J, Wildhaber FD, Strub C, Hall SR, Schmid RA, Geiser T, et al. Towards personalized medicine: chemosensitivity assays of patient lung cancer cell spheroids in a perfused microfluidic platform. Lab Chip. 2015; 15(14):3076–85. https://doi.org/10.1039/c5lc00454c PMID: 26088102

44. Watters KM, Bajwa P, Kenny HA. Organotypic 3D Models of the Ovarian Cancer Tumor Microenvironment. Cancers. 2018; 10(8). https://doi.org/10.3390/cancers10080265 PMID: 30096959

45. Eetezadi S, Evans JC, Shen YT, De Souza R, Piquette-Miller M, Allen C. Ratio-Dependent Synergism of a Doxorubicin and Olaparib Combination in 2D and Spheroid Models of Ovarian Cancer. Molecular pharmaceutics. 2018; 15(2):472–85. https://doi.org/10.1021/acs.molpharmaceut.7b00843 PMID: 29283581

46. Lee JM, Mhawech-Fauceglia P, Lee N, Parsanian LC, Lin YG, Gayther SA, et al. A three-dimensional microenvironment alters protein expression and chemosensitivity of epithelial ovarian cancer cells in vitro. Laboratory investigation; a journal of technical methods and pathology. 2013; 93(5):528–42. https://doi.org/10.1038/labinvest.2013.41 PMID: 23459371

47. Provencher DM, Lounis H, Champoux L, Tétrault M, Manderson EN, Wang JC, et al. Characterization of four novel epithelial ovarian cancer cell lines. In Vitro Cell Dev Biol Anim. 2000; 36(6):357–61. https://doi.org/10.1290/1071-2690(2000)036<0357:COFNEO>2.0.CO;2 PMID: 10949993

48. Astolfi M, Péant B, Lateef MA, Rousset N, Kendall-Dupont J, Carmona E, et al. Micro-dissected tumor tissues on chip: an ex vivo method for drug testing and personalized therapy. Lab Chip. 2016; 16 (2):312–25. https://doi.org/10.1039/c5lc01108f PMID: 26659477

49. Tanyeri M, Tay S. Viable cell culture in PDMS-based microfluidic devices. Methods in cell biology. 2018; 148:3–33. https://doi.org/10.1016/bs.mcb.2018.09.007 PMID: 30473072

50. Sokolova E, Kutova O, Grishina A, Pospelov A, Guryev E, Schulga A, et al. Penetration Efficiency of Antitumor Agents in Ovarian Cancer Spheroids: The Case of Recombinant Targeted Toxin DARPin-LoPE and the Chemotherapy Drug, Doxorubicin. Pharmaceutics. 2019; 11(5). https://doi.org/10.3390/pharmaceutics11050219 PMID: 31067739

51. Mikhail AS, Eetezadi S, Allen C. Multicellular tumor spheroids for evaluation of cytotoxicity and tumor growth inhibitory effects of nanomedicines in vitro: a comparison of docetaxel-loaded block copolymer micelles and Taxotere(R). PloS one. 2013; 8(4):e62630. https://doi.org/10.1371/journal.pone.0062630 PMID: 23626842

52. Kurman RJ, Shih Ie M. The Dualistic Model of Ovarian Carcinogenesis: Revisited, Revised, and Expanded. The American journal of pathology. 2016; 186(4):733–47. https://doi.org/10.1016/j.ajpath.2015.11.011 PMID: 27012190

53. Naora H, Montell DJ. Ovarian cancer metastasis: integrating insights from disparate model organisms. Nature reviews Cancer. 2005; 5(5):355–66. https://doi.org/10.1038/nrc1611 PMID: 15864277

54. Barbolina MV, Adley BP, Kelly DL, Shepard J, Fought AJ, Scholtens D, et al. Downregulation of connective tissue growth factor by three-dimensional matrix enhances ovarian carcinoma cell invasion. International journal of cancer. 2009; 125(4):816–25. https://doi.org/10.1002/ijc.24347 PMID: 19382180

55. Sodek KL, Ringuette MJ, Brown TJ. Compact spheroid formation by ovarian cancer cells is associated with contractile behavior and an invasive phenotype. International journal of cancer. 2009; 124 (9):2060–70. https://doi.org/10.1002/ijc.24188 PMID: 19132753

56. Iwanicki MP, Davidowitz RA, Ng MR, Besser A, Muranen T, Merritt M, et al. Ovarian cancer spheroids use myosin-generated force to clear the mesothelium. Cancer discovery. 2011; 1(2):144–57. https://doi.org/10.1158/2159-8274.CD-11-0010 PMID: 22303516

57. Shuford S, Wilhelm C, Rayner M, Elrod A, Millard M, Mattingly C, et al. Prospective Validation of an Ex Vivo, Patient-Derived 3D Spheroid Model for Response Predictions in Newly Diagnosed Ovarian Cancer. Sci Rep. 2019; 9(1):11153. https://doi.org/10.1038/s41598-019-47578-7 PMID: 31371750

58. Niero EL, Rocha-Sales B, Lauand C, Cortez BA, de Souza MM, Rezende-Teixeira P, et al. The multiple facets of drug resistance: one history, different approaches. Journal of experimental & clinical cancer research: CR. 2014; 33:37. https://doi.org/10.1186/1756-9966-33-37 PMID: 24775603

59. Toepke MW, Beebe DJ. PDMS absorption of small molecules and consequences in microfluidic applications. Lab Chip. 2006; 6(12):1484–6. https://doi.org/10.1039/b612140c PMID: 17203151

60. Zaman MH. The role of engineering approaches in analysing cancer invasion and metastasis. Nature reviews Cancer. 2013; 13(8):596–603. https://doi.org/10.1038/nrc3564 PMID: 23864050